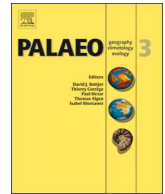




ELSEVIER

Contents lists available at ScienceDirect

Palaeogeography, Palaeoclimatology, Palaeoecology

journal homepage: www.elsevier.com/locate/palaeo

A multi-proxy palaeolimnological record of the last 16,600 years from coastal Lake Kushu in northern Japan



Mareike Schmidt^{a,*}, Christian Leipe^{a,b}, Fabian Becker^c, Tomasz Goslar^{d,e}, Philipp Hoelzmann^c, Jens Mingram^f, Stefanie Müller^g, Rik Tjallingii^f, Mayke Wagner^g, Pavel E. Tarasov^{a,*}

^a Institute of Geological Sciences, Paleontology, Freie Universität Berlin, Malteserstr. 74-100, 12249 Berlin, Germany

^b Nagoya University, Institute for Space-Earth Environmental Research (ISEE), Research Institutes Building II, Furo-cho, Chikusa-ku, Nagoya 464-8601, Japan

^c Institute of Geographical Sciences, Physical Geography, Freie Universität Berlin, Malteserstr. 74-100, 12249 Berlin, Germany

^d Faculty of Physics, Adam Mickiewicz University, Umultowska, 85, Poznan, Poland

^e Poznan Radiocarbon Laboratory, Foundation of the A. Mickiewicz University, Rubież 46, Poznan, Poland

^f Helmholtz Centre Potsdam, GeoForschungsZentrum, Telegrafenberg, 14473 Potsdam, Germany

^g Eurasia Department and Beijing Branch Office, German Archaeological Institute, Im Dol 2-6, 14195 Berlin, Germany

ARTICLE INFO

Keywords:

Diatoms

X-ray fluorescence

Non-pollen palynomorphs

Microfacies

Holocene Optimum

Hunter-gatherer occupation

ABSTRACT

Based on diatom, aquatic pollen and non-pollen palynomorph (NPP), lake sediment microfacies, and X-ray fluorescence (XRF) analyses we define three main phases of lake basin development including a marshy phase (ca. 16,600–9400 cal. yr BP), lagoon phase (ca. 9400–5900 cal. yr BP) and freshwater lake phase (since ca. 5900 cal. yr BP). Marine influence on the lake system linked to global sea-level rise and the Holocene marine transgression reached a maximum between ca. 8000 and 6000 cal. yr BP. An increase of *Aulacoseira subarctica* at 5530 cal. yr BP marks the end of the Holocene Thermal Optimum (i.e. onset of Middle Holocene cooling) in the study region. Our results further suggest that freshwater Lake Kushu had a significant effect on the initial habitation of Rebus Island by sedentary hunter-gatherer populations. The reconstructed onset of stable freshwater conditions (ca. 5100 cal. yr BP) coincided with the appearance of the earliest permanent settlements during the Middle Jomon culture phase (ca. 5000–4000 cal. yr BP). On the other hand, there is evidence for human-induced changes in the limnological conditions. This includes enhanced sediment and nutrient input into Lake Kushu resulting in high eutrophication levels that caused strongly reduced diatom productivity and enhanced green algae growth, which can be attributed to human activities apparently associated with the Okhotsk (ca. 1450–950 cal. yr BP) and Classic Ainu (ca. 350–100 cal. yr BP) culture periods.

1. Introduction

The sediment core RK12 from Lake Kushu on Rebus Island (Fig. 1) analyzed in the current study was obtained under the framework of the Baikal-Hokkaido Archaeology Project (BHAP: <http://bhap.artsrn.uAlberta.ca/>). This international multi-disciplinary research initiative aims at investigating Holocene hunter-gatherer culture dynamics, variability, and resilience and their causal driving factors including possible relations to climate and environmental changes in two regions of the world: Lake Baikal in Russian Siberia and Hokkaido in northern Japan (Tarasov et al., 2013; Weber et al., 2013). Rebus Island in the northern Sea of Japan has been chosen as one of the key study areas in the latter region.

First palaeoenvironmental studies (Kumano et al., 1990; Sato et al., 1998) on the Lake Kushu basin were based on a sediment core extracted

from the mire in the River Oshonnai delta south of contemporary Lake Kushu (Fig. 1D). These works present coarse-resolution records of diatoms and sulfur content providing rough information about the evolution of the lake system. The BHAP focuses on high-resolution, chronologically well-constrained analyses of the RK12 core representing the Lake Kushu lacustrine sedimentary succession. Pilot studies (Müller et al., 2016; Schmidt et al., 2016) have tested and approved the high potential of RK12 to serve these aims and to allow reconstructing past variations in vegetation and climate conditions as well as the evolution of the lake system over the past ca. 16,600 years. Recently, BHAP members have presented a high-resolution terrestrial pollen record from the RK12 core spanning the last 6000 years, which was employed to reconstruct vegetation and climate changes and human–environment interactions on the island (Leipe et al., 2017; Leipe et al., 2018).

Regarding the prehistory of Rebus Island, the record of regional

* Corresponding authors.

E-mail addresses: mareike.schmidt22@gmail.com (M. Schmidt), ptarasov@zedat.fu-berlin.de (P.E. Tarasov).

<https://doi.org/10.1016/j.palaeo.2018.11.010>

Received 23 August 2018; Received in revised form 9 November 2018; Accepted 10 November 2018

Available online 12 November 2018

0031-0182/ © 2018 Elsevier B.V. All rights reserved.

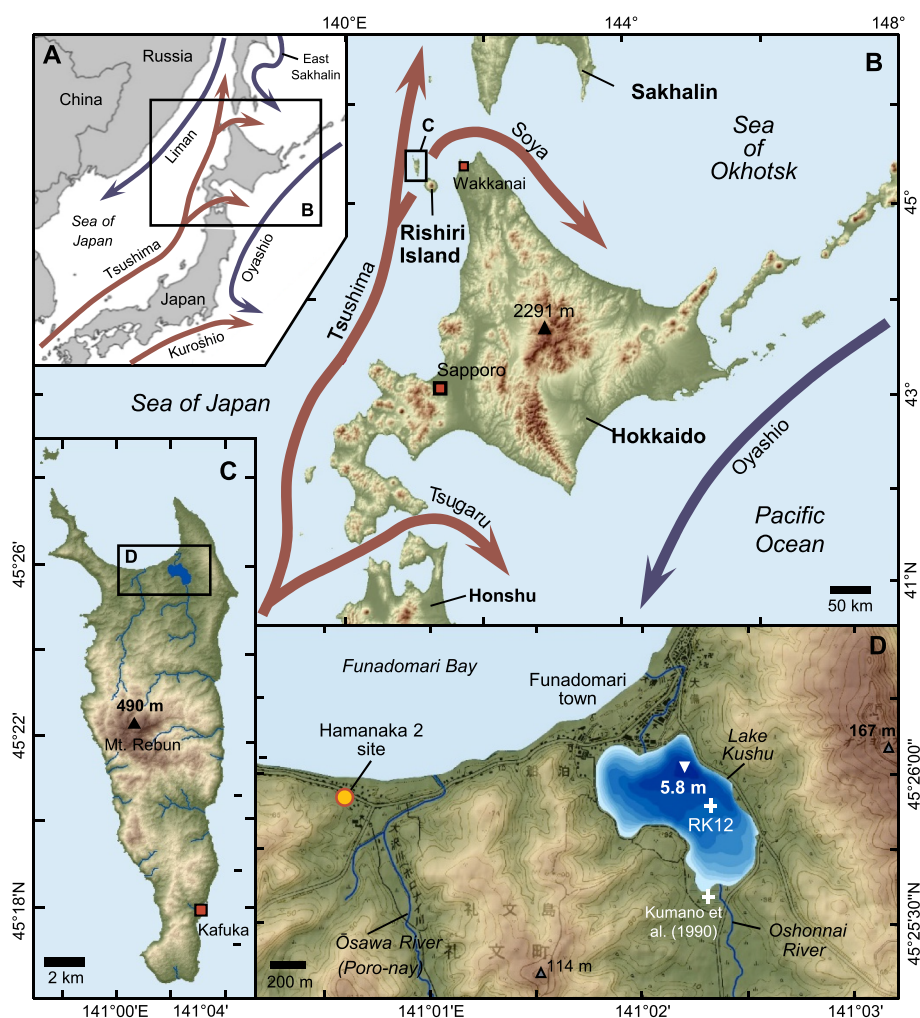


Fig. 1. Chart compilation showing (A) the location of the Hokkaido Region in the NW Pacific; (B) the location of Rebut Island in the Sea of Japan with main cold (blue) and warm (red) sea surface currents around Hokkaido; (C) a topographic map with main streams on northern Rebut Island; and (D) the outline and bathymetry of Lake Kushu in 0.5 m steps (according to T. Haraguchi, Osaka City University). The white cross marks the location of Kushu core RK12. The topographic maps are based on elevation Shuttle Radar Topography Mission (SRTM) v4.1 data (Reuter et al., 2007; Jarvis et al., 2008). Isolines in (D) derive from a topographic map (Geospatial Information Authority of Japan, 2012). (For interpretation of the references to color in this figure legend, the reader is referred to the web version of this article.)

archaeological surveys (Abe et al., 2016) assigns the earliest presence of humans to the late Palaeolithic (Abe et al., 2016) dating sometime between 20,000 and 11,000 cal. yr BP (Inui, 2000). However, the first residential sites appeared much later during the Neolithic Middle Jomon period ca. 5000–4000 cal. yr BP (Weber et al., 2013; Müller et al., 2016; Abe et al., 2016). This raises the following questions: (i) what could be the reason for such a relatively late occurrence of permanent habitation, (ii) can a multi-proxy study help to understand past environmental changes in the lake area and test whether they are correlated to registered prehistoric cultural dynamics, (iii) which role Lake Kushu played in the human occupation history of Rebut Island, and (iv) have the past human inhabitants impacted the lake system, leaving traces in its sedimentary record?

The current study uses diatom, aquatic pollen and non-pollen palynomorph (NPP), microfacies, and X-ray fluorescence (XRF) analyses applied to the RK12 core sediment to reconstruct lake system dynamics since ca. 16,600 cal. yr BP. We provide a detailed and robustly-dated palaeolimnological record to facilitate regional palaeoclimatic and palaeoenvironmental interpretations for the lateglacial–Holocene time interval. We conducted a multi-proxy analysis on a 90-cm-long finely laminated sediment section of RK12 dating to the middle Holocene to enhance interpretation of different environmental indicators and to detect lake system fluctuation on a bi-decadal to seasonal scale. We discuss our results considering potential signals for human–environment interactions in relation to Lake Kushu in light of available information on the local/regional prehistory and previous palaeoenvironmental studies.

2. Regional settings

Lake Kushu (45°25′58″N, 141°02′05″E, ca. 4 m above sea level, a.s.l.) is a coastal freshwater lake in the northern part of volcanic Rebut Island situated in the northern Sea of Japan (Kimura, 1997; Goto and McPhie, 1998, Fig. 1A–C). The lake has a maximum depth of 5.8 m and a catchment area of about 10 km² (Müller et al., 2016; Schmidt et al., 2016) and is separated from Funadomari Bay by a sand dune of ~400 m width and ~15 m height (Sato et al., 1998; Schmidt et al., 2016). The Oshonnai River enters the lake in the south and an outflow in the north connects the lake with Funadomari Bay (Fig. 1D).

The modern climate in the study region is mostly controlled by the East Asian monsoon system and the seasonal migration of the East Asian polar front (Leipe et al., 2013 and references therein). During the cold half of the year (November–April), the region is mainly influenced by north-western air masses (East Asian winter monsoon, EAWM). The Tsushima Warm Current (TWC) (Fig. 1B) induces relatively warm conditions in the eastern part of the Sea of Japan leading to relatively mild winters and high amounts of snowfall in the western part of the Hokkaido region (Igarashi, 2013). The atmospheric circulation of the warm season (May–October) is mainly controlled by south-eastern winds of the East Asian summer monsoon. The mean monthly air temperature on Rebut Island varies between –6.4 °C in January and 19.4 °C in August, the mean annual precipitation is 1102 mm, with highest amounts falling from September (131 mm) to December (106 mm) (see Schmidt et al., 2016 for details). The generally high annual moisture availability promotes a dense vegetation cover with

predominantly cool temperate and boreal woody plants (Müller et al., 2016). Human-induced deforestation of Rebus Island in the early-mid 20th century CE caused the spread of dwarf bamboo, knotweed, and other herbaceous plants, which hamper the re-establishment of forest vegetation (Müller et al., 2016). However, nature conservation efforts and incorporation of the island into the Rishiri Rebus Sarobetsu National Park has supported the spread of natural-vegetation-dominated areas during last decades.

3. Material and methods

3.1. Core RK12 and chronology

Drilling of two parallel sediment cores (RK12-01 and RK12-02) was performed in February 2012 at 5.8 m water depth in the central part of Lake Kushu (Fig. 1D). Combining both cores resulted in a 19.5-m-long continuous composite sedimentary succession (RK12) whose lithology is described in detail in Müller et al. (2016). The age–depth model (Fig. 2) was constructed using a set of 57 AMS ^{14}C datings of bulk sediment samples (each representing 1 cm of core depth) and the free-shape algorithm (Goslar et al., 2009). Fig. 2 shows age–depth relations in the upper half of the core accumulated during the past 6000 years (Müller et al., 2016). The lower core section contains several samples, which show too old ages resulting in distinct reversals in the age–depth curve. These samples are obviously affected by contamination of older material and thus were excluded from model construction. Robustness of the age model for the upper part of the RK12 core is supported by tephrostratigraphical correlation with the Millennium (B-Tm) eruption of Changbaishan Volcano in northeastern China (Chen et al., 2016) and the correlation between the RK12 pollen record and the AMS-dated archaeobotanical assemblages from the nearby archaeological site Hamanaka 2 (Fig. 1D) presented by Leipe et al. (2018). Müller et al. (2016) also demonstrated a good temporal correlation between the

lateglacial/early Holocene part of the RK12 pollen record and the regional pollen-based stratigraphy (Igarashi and Zharov, 2011; Nakagawa et al., 2005). According to the derived chronology, the sedimentation rate is generally high with on average ca. 0.5 mm/yr between 19.5 and 16 m depth (ca. 16,600–9500 cal. yr BP) and ca. 1.7 mm/yr between 16 and 0.5 m depth (ca. 9500–270 cal. yr BP). The detailed multi-proxy study including diatom, pollen, microfacies, and XRF analyses was performed on a 90-cm sequence of core section RK12-02-9 covering the composite depth of 848–938 cm (ca. 5600–5200 cal. yr BP) showing sedimentation rates of ca. 1.3–1.4 mm/yr (848–878 cm), ca. 2 mm/yr (878–888 cm), and ca. 5 mm/yr (888–938 cm).

3.2. Diatom analysis

Samples for diatom analysis were extracted at an interval of 8 cm from the RK12 sediment sequence and every 2–3 cm from section RK12-02-9. The 1-cm-thick sediment samples were prepared according to the standard preparation method (Battarbee et al., 2001) using 37% HCl and 10% H_2O_2 to remove carbonates and organic residuals, respectively (see Schmidt et al., 2016 for details). The prepared diatom concentrates were embedded in Naphrax™ and counted using a light microscope at 1000 \times magnification and immersion oil. A minimum of 300 valves were counted per sample. Taxa were identified using the guides of Krammer and Lange-Bertalot (1997, 1999, 2000, 2004), Ohtsuka (2002), Kobayasi et al. (2006), Levkov (2009), Houk et al. (2010), Lee (2011, 2012), and Tanaka (2014). Taxa names are based on the taxonomy provided on the website AlgaeBase (Guiry and Guiry, 2015). Diatom abundances are presented in percentage diagrams (Figs. 3A and 7A). The planktonic to benthic ratio (P/B) was calculated by dividing the sum of planktonic valves by the sum of total valve counts. The stack diagrams for salinity, trophic, and pH and the P/B ratios (Fig. 4) were plotted with Tilia® software (Grimm 1991–2011), using known taxon-specific ecological optima (see Schmidt et al., 2016 for details). The local diatom zones (LDZ) and subzones (LDSZ) were defined using the CONISS (Constrained Incremental Sum of Squares) function in the Tilia® software (Grimm 1991–2011; Fig. 4) for stratigraphically constrained cluster analysis.

3.3. Pollen and non-pollen palynomorph analysis

To support the interpretation and discussion of the Lake Kushu aquatic system development, we analyzed aquatic plant pollen, green algae colonies, and other non-pollen palynomorphs (NPPs) contained in the RK12 sediments. Samples of 1 cm³, each representing a depth section of 1 cm, were collected every 3 to 4 cm from the cleaned core surface and processed following standard procedures (Cwynar et al., 1979; Fægri et al., 1989), including 7- μm ultrasonic fine sieving, hydrofluoric acid treatment, and acetolysis. Two tablets of *Lycopodium* marker spores (batch no. 177745), each containing $18,584 \pm 370$ spores, were added to each sediment sample prior to the chemical treatment for calculating concentrations of identified palynomorphs (Stockmarr, 1971). Water-free glycerol was used for sample storage and preparation of microscopic slides. Taxa were counted at magnifications of 400 \times and 600 \times , with the aid of published identification keys and atlases (Shimakura, 1973; Nakamura, 1980a, 1980b; Reille, 1992, 1995, 1998; Beug, 2004; Miyoshi et al., 2011; Demske et al., 2013). For all analyzed samples, percentages of aquatic plant pollen and NPPs were calculated using the total terrestrial pollen sum plus the sum of palynomorphs in the respective group. The Tilia® software (Grimm 1991–2011) was used for calculating pollen and NPP taxa percentages and drawing diagrams (Figs. 3B and 7).

3.4. Semi-continuous X-ray fluorescence (XRF) analysis

The semi-continuous elemental analysis was performed on a Thermo Scientific Niton XL3t portable energy-dispersive X-ray

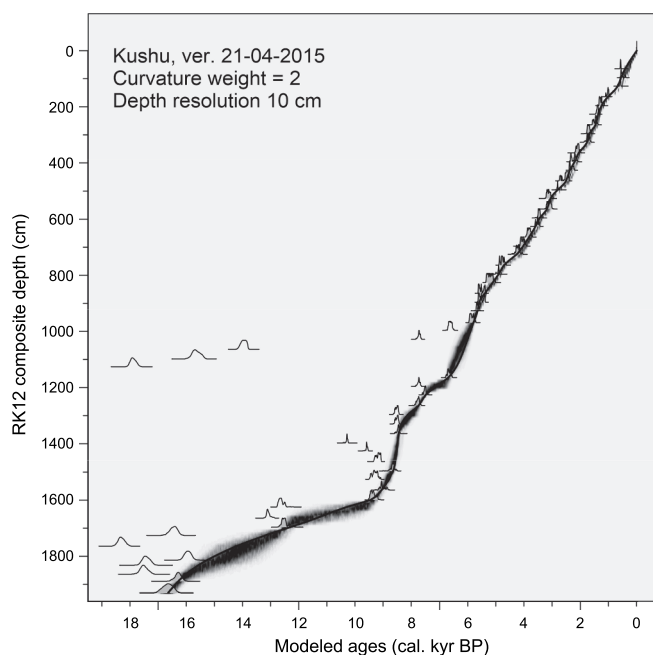


Fig. 2. Age–depth model (best-fit line with uncertainty ranges) for the RK12 sediment core from Lake Kushu constructed using the free-shape algorithm (Goslar et al., 2009). Radiocarbon dates were converted to calendar ages using the Intcal13 calibration curve (Reimer et al., 2013). Grey silhouettes along the best-fit line represent calibrated ^{14}C dates considered by the model, while the non-filled silhouettes left of the best-fit line represent older ^{14}C dates rejected by the model.

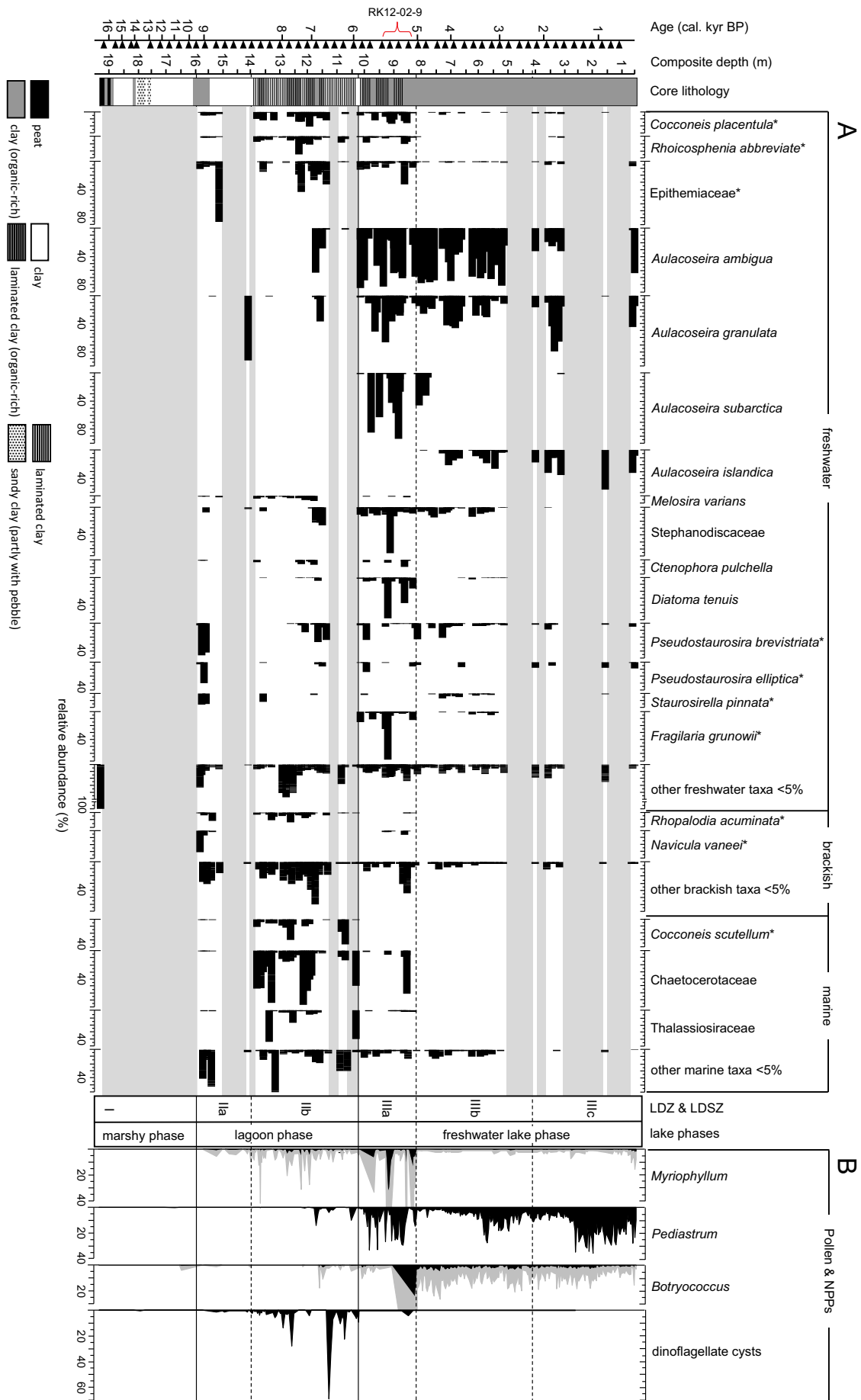


Fig. 3. Percentage diagrams showing abundances of selected (A) diatoms as well as (B) aquatic pollen and NPPs (shaded areas show 5-times exaggeration) from the Lake KUSHU RK12 sediment core. Diatoms are grouped into freshwater, brackish, and marine taxa and taxa that contribute < 5% to a sample assemblage are grouped into ‘other freshwater taxa’, ‘other brackish taxa’, and ‘other marine taxa’. Benthic diatom taxa are differentiated from planktonic taxa by an asterisk. Red curly bracket indicates the position of section RK12-02-9 (Figs. 7 and 8). Grey bars illustrate eight main sequences in which no or < 300 diatoms per sample were detected (see Chapter 4.1.1 for details). Triangles along the age axis indicate AMS datings (n = 57) used to build the age-depth model (Müller et al., 2016). (For interpretation of the references to color in this figure legend, the reader is referred to the web version of this article.)

fluorescence spectrometer (p-ED-XRF) in ‘mining mode’ for (in-device) fundamental parameter calibration. Analysis was done core segment-wise (i.e. on 1-m core segments) with the sediment surface covered with cling film and transferred into a sample chamber mounted onto an ASC® manual core track and analyzed in 1-cm steps for calcium (Ca), chlorine (Cl), iron (Fe), potassium (K), silicon (Si), strontium (Sr), titanium (Ti), and vanadium (V) according to Hoelzmann et al. (2017). Only measurements that show values larger than four times the 1-σ errors were considered. The two certified lacustrine sediments LKSD-2 (lake sediment; Lot. Nr. 688) and LKSD-4 (lake sediment; Lot. Nr. 897) (Lynch, 1990) were used as reference material (CRM) for quality control (Ca, Fe, K, Si, Sr, Ti). Recovery values for both CRMs are shown in Supplementary material S1. To assure constant measurement conditions the CRMs were measured at the beginning and end of each core

segment analysis.

Elemental data was analyzed using a compositional data approach to manage the consistent sum-constrained model (Aitchison, 1986). For a more objective interpretation of the multivariate data and to allow for comparison of the geochemical data with LDZ, we grouped the data in geochemical units (‘chemofacies’) based on a hierarchical cluster analysis (e.g. Templ et al., 2008; Montero-Serrano et al., 2010 for compositional examples). Analysis was performed in R (R Core Team, 2013) using the *compositions* v1.40–1 (van den van den Boogaart et al., 2014), the *zCompositions* (Palarea-Albaladejo and Martín-Fernández, 2015), and the *rioja* v0.9-6 (Juggins, 2015) packages. A detailed description of the procedure as well as raw data, interim results, and the computation code is provided in Supplementary material S2.

Firstly, missing values (values below detection limit) were imputed

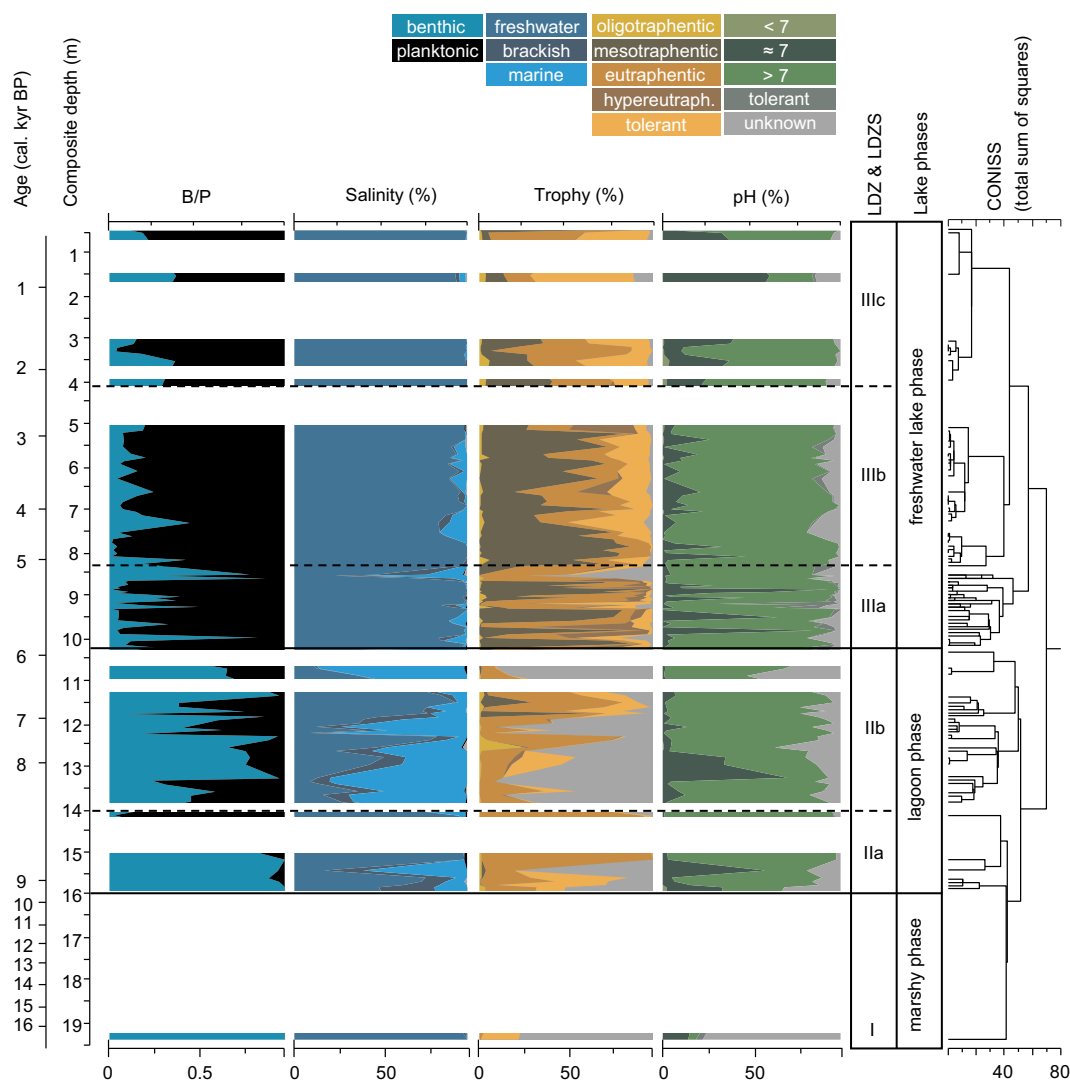


Fig. 4. The diagrams show the reconstructed ecological parameters P/B, salinity, trophy, and pH, based on autecology information calculated with Tilia® software (Grimm 1991–2011). Gaps represent eight main sections with samples containing no diatoms or less than the minimum count number of 300 valves (see Chapter 4.1.1 for details).

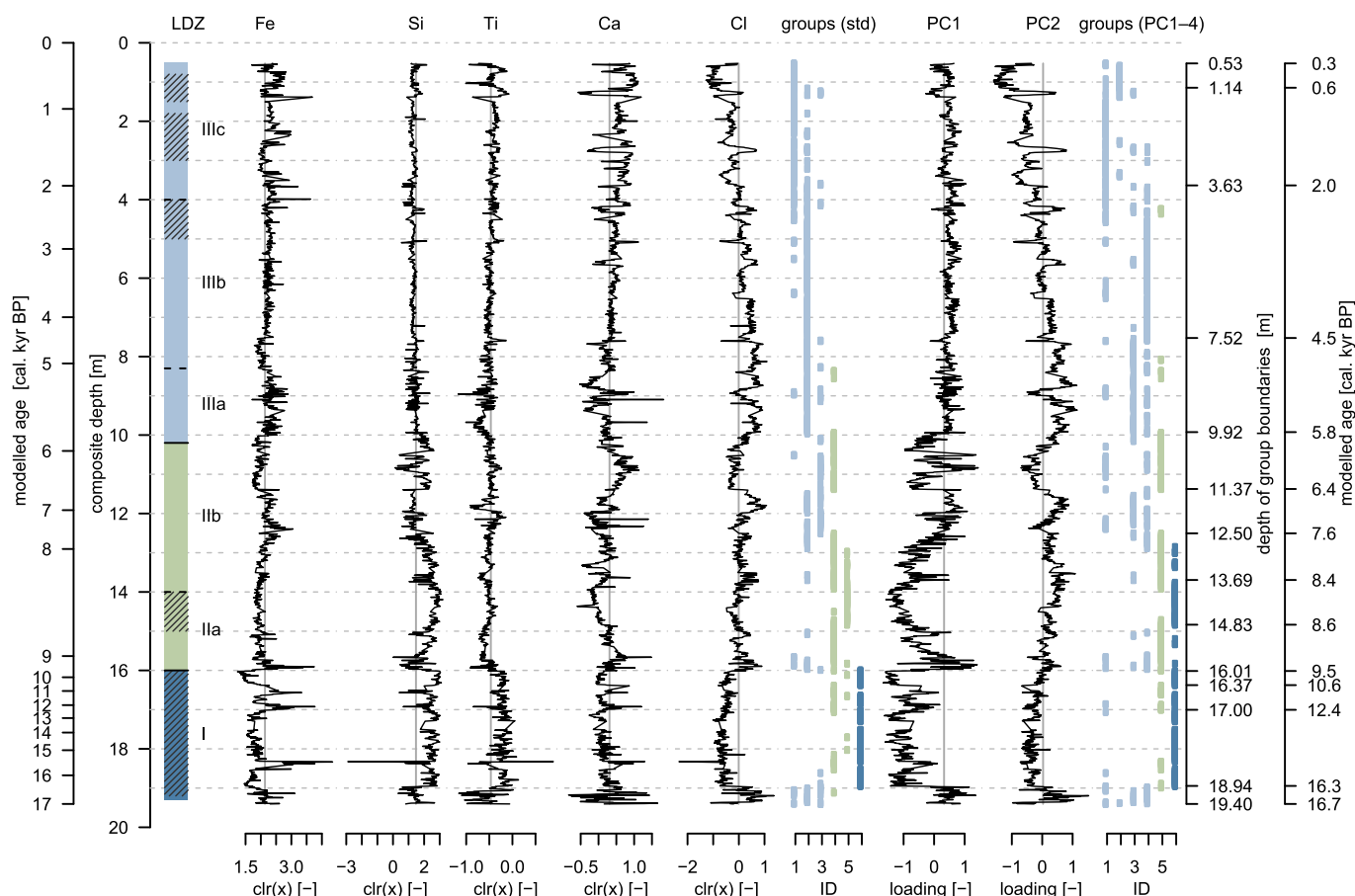


Fig. 5. The geochemical record of RK12: Age/depth vs. local diatom zones (LDZ) and subzones (LDSZ), centered log-ratio (clr) transformed contents of selected elements, groups obtained by hierarchical cluster analysis of standardized element contents (std), and the first four principal components (PC). The secondary y-axis shows the boundaries (age/depth) of groups obtained by the depth-constrained cluster analysis of geochemical data. Geochemical groups are shown in the same color as the most similar lake evolutionary stages (see Fig. 6, PCA). Groups: 1, 2, and 3 = freshwater; 4 = lagoon (std) or freshwater (PC1–4); 5 = lagoon; and 6 = marsh. Hatched areas in the LDZ chart mark main core sections in which no or < 300 diatoms per sample were detected.

using multiplicative lognormal replacement (Palarea-Albaladejo and Martín-Fernández, 2013) to allow for data transformation. Secondly, the data were centered log-ratio (clr) transformed.

The clr is defined as

$$z = clr(x) = [\ln(x_1/g(x)), \ln(x_2/g(x)), \dots, \ln(x_D/g(x))], \quad (1)$$

where $g(x) = [x_1 \cdot x_2 \cdot \dots \cdot x_D]^{1/D}$ is the geometric mean of all parts of the observation $x = [x_1, x_2, \dots, x_D]$. Subsequently, potential outlier (values greater/smaller than the median $M \pm 3 \times$ the absolute median deviation MAD of the neighboring observations, $k = 25$ cm) was replaced by a running median ($k = 5$ cm). The third step is used to normalize the variability and value range of major, minor, and trace elements. This includes the standardization of the data using a robust z-transformation (center = M , scale = MAD) or reduction of the dimensionality of the data using a principal component analysis (PCA) of clr-transformed data.

The robust z-transformation is defined as

$$M - 3 \times MAD < x_i < M + 3 \times MAD, \quad (2)$$

where $M(j)$ is the median of all parts and

$$MAD = b M_i (|x_i - M_j(x_j)|). \quad (3)$$

In the Eqs. (2) and (3), MAD is the median absolute deviation and x_j is the n original observations. We performed the cluster analysis of Manhattan distances applying Ward's method (hierarchical clustering; e.g. Strauss and von Maltitz, 2017) and CONISS (Grimm, 1987) for depth-constrained clustering (Gill et al., 1993). The number of clusters

is based on the different lithologies and the number of LDZ ($g = 6$). The interpretation of the chemofacies is based upon the LDZs (Figs. 5 and 6).

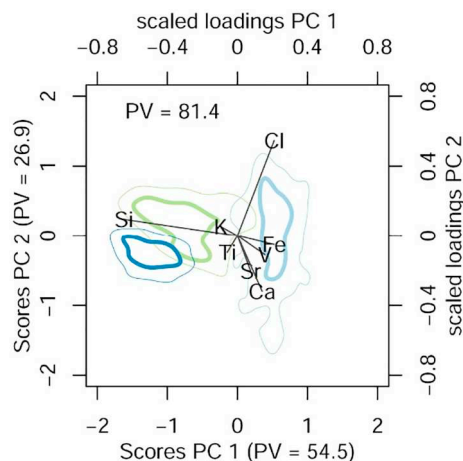


Fig. 6. PCA biplot with polygons that mark the 50% (bold lines) and 95% distribution of observations. The colors indicate cluster interpretation according to the local diatom zones (LDZ): dark blue = LDZ I; green = LDZ II; light blue = LDZ III, PV = Proportion of Variance [%]. (For interpretation of the references to color in this figure legend, the reader is referred to the web version of this article.)

3.5. Microfacies analysis

Thin sections for microfacies analysis were prepared from the RK12-02-9 segment covering the composite depth of 848–938 cm. Nine 10-cm-long slices were continuously extracted from the fresh sediment core surface following standard procedures including freeze-drying and impregnation with epoxy resin (Brauer and Casanova, 2001). Microfacies analysis was performed using petrographic microscopes with visual light (Nikon SMZ-U for low magnification, and Olympus BX53 for high magnification). The lamination types were classified based on microscopic observation of individual sediment layers and sub-layers as well as careful definition of the layer boundaries. Images (Fig. 8) were taken using a digital camera mounted onto the microscopes and processed with the cellSens Dimension© 1.5 software (Olympus Corporation, 2011).

4. Results and interpretations

4.1. Diatoms and lithology

4.1.1. RK12 composite core

The results of the diatom analysis are summarized in Figs. 3A and 4. We identified 182 taxa including 33 planktonic and 149 benthic species. Of the 210 analyzed samples 106 contain no diatoms or less than the minimum count number of 300 valves. Visual presentation outlines that the latter samples mainly cluster in eight core sections including depth intervals 1924.0–1583.5, 1511.5–1416.5, 1408.5–1384.5, 1058.5–1033.5, 494.5–407.5, 399.5–369.5, 312.0–161.5, and 154.0–62.5 cm (Figs. 3A and 4). The obtained diatom record allows refining the boundaries of the three lake phases (marshy, lagoon, and freshwater) defined in Schmidt et al. (2016). The transition from the marshy to lagoon phase is detected at 1600 cm depth (ca. 9400 cal. yr BP) and the shift from the lagoon to freshwater phase is evident at 1020 cm (ca. 5900 cal. yr BP). The high-resolution diatom record further allows for defining the following LDZs and LDSZs.

The bottom part of the record (prior to 1600 cm) represents the ‘marshy phase’ (Schmidt et al., 2016). However, diatoms are only found in the lowermost layers (LDZ I, 1935–1900 cm; 16,600–16,250 cal. yr BP). The diatom assemblage of these three samples contains valves of freshwater *Diploneis subovalis* Cleve (43–78%), *Pinnularia viridis* (Nitzsch) Ehrenberg (15–20%), *Pinnularia episcopalis* Cleve (0–13%), and *Cymbella aspera* (Ehrenberg) Cleve (3–13%) (see Schmidt et al., 2016 for details). *D. subovalis* and *P. viridis* are benthic taxa common in running waters (Krammer and Lange-Bertalot, 1997) and stream-fed ponds at ca. 5 cm water depth (Harper, 1976), respectively. The diatom assemblage composition in concert with the core lithology (i.e. peat and organic rich clay) and high values of Cyperaceae pollen reaching ca. 60% of the total pollen sum (Müller et al., 2016) suggest swampy, shallow-water conditions. The above layers (1900–1600 cm; 16,250–9400 cal. yr BP) represented by clay and sandy clay partly with pebbles are marked by extremely low diatom counts (i.e. single valves) or entire absence of diatoms. The pollen record (Müller et al., 2016) demonstrates decreasing but still high percentages of Cyperaceae (10–60%) and relatively high percentages of Poaceae (10–20%) pollen and Polypodiaceae fern spores (10–15%), likely representing coastal semi-aquatic environments. We interpret this as evidence for an interval of unstable water conditions (and shallow, possibly tidal environments) due to a rising sea level, which is best described by a marshy phase, a transitional interval between the swampy and lagoon phases.

LDZ II (1600–1020 cm; 9400–5900 cal. yr BP) marks the lagoon phase and can be subdivided into two subzones LDSZ IIa and b. The organic-rich sediments in LDSZ IIa (1600–1390 cm; 9400–8400 cal. yr BP) are mostly composed of benthic freshwater diatoms in the lower part. Clayey sediments with little organic content and absence of valves characterize the upper part of LDSZ IIa. LDSZ IIb (1390–1020 cm; 8400–5900 cal. yr BP) shows highest percentages of marine Chaetocerotaceae resting spores

(≤80%). The lithology is characterized by laminated, partly organic-rich clay. A short interval between 1180 and 1130 cm shows freshwater diatoms such as *Aulacoseira ambigua* (Grunow) Simonsen (65%) and *A. granulata* (Ehrenberg) Simonsen (40%), *Pseudostaurosira brevistriata* (Grunow) Williams & Round (≤28%), and the absence of marine frustules.

LDZ III (1020–50 cm; 5900–270 cal. yr BP) corresponds to the freshwater lake phase and can be divided into three subzones. The partly laminated organic-rich sediments in LDSZ IIIa (1020–830 cm; 5900–5100 cal. yr BP) show a decrease of marine diatoms (≤5%) and increase of freshwater *A. ambigua* (≤85%), *A. granulata* (Ehrenberg) Simonsen (≤65%), *A. subarctica* (Müller) Haworth (≤96%), Epithemiaceae (≤35%) and Stephanodiscaceae (≤67%), and brackish taxa (60%) as well. One peak of marine Chaetocerotaceae resting spores occurs at 850 cm (60%). The lithological analysis in LDSZ IIIb (830–410 cm; 5100–2200 cal. yr BP) reveals organic-rich clay without lamination. The diatom assemblages are mainly composed of freshwater *A. ambigua* (≤84%), *A. granulata* (≤50%), *A. islandica* (≤24%), Stephanodiscaceae (≤15%), and *P. brevistriata* (≤20%). The non-laminated, organic-rich sediments in LDSZ IIIc (410–50 cm; 2200–270 cal. yr BP) are characterized by the absence of diatom valves in most parts. Fewer samples contain valves mainly consisting of planktonic freshwater *A. ambigua* (≤64%), *A. granulata* (≤78%) and *A. islandica* (≤56%, Fig. 3A).

4.1.2. Section RK12-02-9

The 22 analyzed samples of section RK12-02-9 (938–848 cm; 5600–5200 cal. yr BP, Fig. 7) contain high amounts of well-preserved diatoms, which allowed counting of at least 500 valves per sample. In total, 100 species of 52 genera and 27 families have been identified. The assemblages show the dominance of benthic (n = 84) over planktonic (n = 16) forms. The CONISS analysis delimited five local diatom zones (LDZ-9 I-V), which are described in the following paragraphs.

LDZ-9 I (938–928 cm; 5640–5610 cal. yr BP) is comprised of two samples and is dominated by freshwater planktonic *A. ambigua* (≤82%) and *A. granulata* taxa (≤66%), which often co-occur because of similar ecological requirements. Both taxa, which prefer bright light and temperate conditions, bloom in summer and autumn and are mainly found in shallow, alkaline lakes (Rioual et al., 2007). *A. ambigua* prefers meso- to eutrophic conditions (Reynolds, 1998; Rioual et al., 2007; Poister et al., 2012), whereas *A. granulata* occurs in eutrophic lakes with water temperatures excessively higher than 15 °C (Shear et al., 1976). Both taxa require high total phosphorus (TP) and silica concentrations (Rioual et al., 2007).

The three samples of LDZ-9 II (928–917 cm, 5610–5580 cal. yr BP) are characterized by the dominance of freshwater *Fragilaria grunowii* Lange-Bertalot & Ulrich and *Diatoma tenuis* Agardh reaching up to 68% and 58%, respectively. Both taxa are often found in cold, oxygen- and carbon-rich headwaters of streams (Patrick, 1977).

LDZ-9 III (917–867 cm; 5580–5360 cal. yr BP) includes 13 samples that mostly contain the planktonic taxa *A. ambigua*, *A. granulata*, and *A. subarctica*. The lowermost sample of this stage shows a peak in *Cyclotella meneghiniana* Kützing with the frequency reaching 65%. Increasing abundances (from 26 to 93%) of *A. subarctica* are determined from 895 to 886 cm. This taxon is common in shallow (Gibsen et al., 2003), circumneutral (Rioual et al., 2007), nordic (Krammer and Lange-Bertalot, 2000) lakes with seasonal ice cover (Kilham et al., 1996; Interlandi et al., 1999; Gibson and Foy, 1988) that prefers cold-water conditions with favored temperatures about 4 °C (Stoermer and Ladewski, 1976). Three peaks of *A. ambigua* occur at 895 cm (64%), 880 cm (61%), and 873–868 cm (68–71%).

One sample represents LDZ-9 IV (867–864 cm; ca. 5360–5340 cal. yr BP), which is dominated by *Stephanodiscus hantzschii* Grunow (41%) and *D. tenuis* (36%) and marks a shift from the *Aulacoseira* spp. dominated assemblages in LDZ-9 III towards the uppermost zone, which is marked by a substantial abundance of brackish/marine taxa. The high percentages of *S. hantzschii* indicate a nutrient

Fig. 7. Compilation of the high-resolution analyses results of section RK12-02-9 with microfacies; diatom and pollen percentage diagrams; reconstructed autecology based on diatoms; and defined local diatom zones (LDZ-9 I-V). Benthic diatom taxa are differentiated from planktonic taxa by an asterisk.

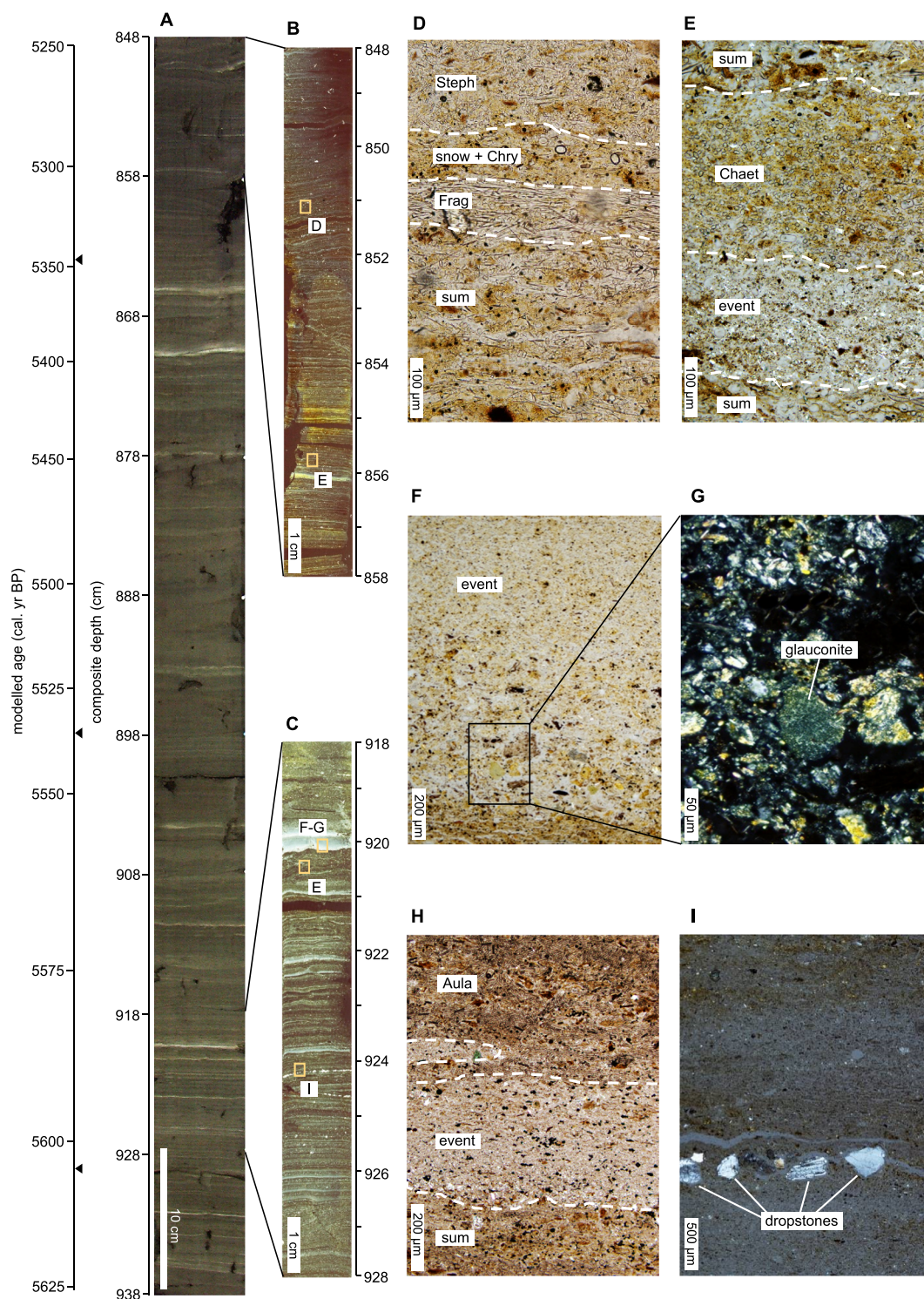


Fig. 8. Images of RK12-02-9 showing (A) an overview photograph of the whole 90 cm section; (B and C) selected thin-section images with yellow rectangles indicating the location of the microscopic images (D–I) with ‘Aula’ representing Aulacoseiraceae bloom, ‘Chaet’ – Chaetocerotaceae resting spores, ‘Chry’ – Chrysophyte cysts, Frag – Fragilariaceae bloom, Steph – Stephanodiscaceae bloom, snow – snowmelt layer, sum – summer layer, and event – event layer. (For interpretation of the references to color in this figure legend, the reader is referred to the web version of this article.)

enriched environment (van Dam et al., 1994).

The uppermost LDZ-9 V (864–848 cm; ca. 5340–5220 cal. yr BP) is marked by a distinct decrease in planktonic freshwater diatoms

compared to LDZ-9 III associated with a change in species composition towards benthic taxa including *Cocconeis placentula* Ehrenberg ($\leq 13\text{--}15\%$), *Rhopalodia gibba* (Ehrenberg) Müller ($\leq 25\%$), and

Rhoicosphenia abbreviata (Agardh) Lange-Bertalot ($\leq 10\%$). Being virtually absent (on average $< 1\%$) in the two previous zones, brackish and marine taxa increase significantly (on average 15 and 25%, respectively).

4.2. Aquatic pollen and NPPs

4.2.1. RK12 composite core

Changes in the relative frequencies of aquatic plant pollen, green algae, and dinoflagellate cysts are partly in line with the defined LDZ and LDSZ (Fig. 3B). Pollen of the water plant *Myriophyllum* (water-milfoil) start to occur in LDSZ IIa, reach maximum abundances in LDSZ IIIa (up to 33%), and decrease in LDSZ IIIb to $< 3\%$. The two green algae *Pediastrum* (35%) and *Botryococcus* (24%) show maximum frequencies in LDSZ IIIa. After several peaks in this zone, *Pediastrum* percentages decrease in LDSZ IIIb to 5% and slowly re-increase to up to 30% above 270 cm depth. After a slight decline towards the end of LDSZ IIIb, they re-increase again in LDSZ IIIc to up to 36%. After a peak at 830 cm (LDSZ IIIa), *Botryococcus* percentages decrease in LDSZs IIIb and IIIc to 3–5%. Dinoflagellate cysts mainly occur in LDSZ IIb with distinct peaks in percentages at 1260 cm (30%) and 1130 cm (67%).

4.2.2. Section RK12-02-9

As observed for most of the RK12 composite sequence, changes in *Myriophyllum* pollen and green algae percentages (Fig. 7) correspond with the diatom zones described in Chapter 4.1.2. With minor presence of *Botryococcus*, occurring at low frequencies (3%) only in two samples (928 and 910 cm), the changes in algae frequencies are mainly associated with *Pediastrum*. In LDZ-9 I *Myriophyllum* percentages start to increase from 1% (933 cm) to 8% (929 cm) paralleled by a strong increase in *Pediastrum* values from 3% to 38% and a subsequent decrease to 18%. In the following diatom zone (LDZ-9 II) *Myriophyllum* reaches maximum values of on average 30%, while *Pediastrum* is marked by low values of on average 5%. The subsequent sections (LDZs-9 III and IV) show a reversed situation. After a short transition, *Myriophyllum* remains on low (6%) and *Pediastrum* on high (30%) average percentages. In the uppermost zone (LDZ-9 V) *Myriophyllum* values remain on low levels (5%), except for a peak (18%) at 860 cm, and *Pediastrum* frequencies decrease and virtually disappear between 860 and 852 cm.

4.3. XRF analysis

The results for Ca, Cl, Fe, K, Si, Sr, Ti, and V from the semi-continuous p-ED-XRF analysis were used to determine and to differentiate the elemental compositions throughout the core. Data are summarized in six different groups by hierarchical cluster analysis and each single observation ($n = 1700$) analysis is attributed to one of the six groups (std) according to the LDZ and LDSZ (Fig. 5). PCA-analysis revealed that 81.4% of the geochemical core composition is explained by loadings of PC1 (54.5%) and PC2 (26.9%). The compositional biplot of PCs 1 and 2 (Fig. 6) shows how specific elements correlate and to which degree the elements contribute to the specific PC. For example, Fe and V as well as Ca and Sr point in similar directions and thus to related characteristics throughout the core. Therefore, Sr and V are not shown in the elemental content summary plot (Fig. 5). For PC1 Si and Fe are the main drivers, whereas Ca, Sr, and Cl mainly represent variations in PC2. The almost perfect orthogonality between Fe-K-Si (PC1) and Ca-Cl-Sr (PC2) shows that these element combinations represent different chemofacies.

4.4. Microfacies of section RK12-02-9

Five descriptive types of sediments were identified ranging from well mixed homogenous to finely laminated sediments with visible annual to seasonal layers (Figs. 7 and 8). Well-laminated sediment sections occur in the lower (926–920 cm) and upper (866–848 cm) parts of RK12-02-9 (Fig. 8A–C). The sediments between (920–866 cm)

exhibit no or only faint lamination. The following main layer types were identified: (1) clastic layers with high portions of terrestrial material (snowmelt spring layer), often containing Chrysophyte cysts (Fig. 8D); (2) diatom bloom layers that consist entirely of valves of *Aulacoseira* sp. (Fig. 8H), Fragilariaceae (Fig. 8D), or *Stephanodiscus* sp. (Fig. 8D); (3) mixed layers with organic residues and diatom valves, sometimes containing *Chaetoceros* spp. resting spores (Fig. 8E); (4) well-sorted clastic layers of different thickness sometimes containing glauconitic grains, secondary dissolved (and partly dissolved) gypsum crystals and/or Chaetocerotaceae spp. resting spores (i.e. event layers) (Fig. 8F and G), and (5) layers with dropstones up to 0.5 mm in diameter (Fig. 8H).

Highest frequencies of *Aulacoseira* sp. layers are found in the indistinctly broad to broad layers (ca. 926–920 cm) (Fig. 8H). Event layers with marine diatoms occur at 926–920 and 856–852 cm (red arrows in Fig. 7) within LDZs-9 II and V. The laminae in the uppermost part of the analyzed section (862–848 cm) are well-pronounced and show highest abundances of *Chaetoceros* spp. layers. The microfacies in this section is characterized by many changes and irregularities regarding layer succession and thickness. Here, a typical annual cycle starts with a clastic snowmelt spring layer partly accompanied by Chrysophyte cysts or dropstones, followed by a spring diatom bloom layer, a summer mixed layer, and a fall diatom bloom layer with valves of *Aulacoseira* sp., Fragilariaceae, or *Stephanodiscus* sp.

5. Discussion

5.1. Lake basin evolution, hydrological conditions, and human activities

The obtained multi-proxy data allow for detailed reconstruction of the development as well as hydrological conditions of Lake Kushu and add information to the discussion of human-environmental interactions on Rebus Island (Müller et al., 2016; Schmidt et al., 2016; Leipe et al., 2017; Leipe et al., 2018). Based on the high-resolution diatom, aquatic pollen and NPP, and p-ED-XRF chemofacies records, we refine the timing of the detected three lake evolutionary intervals since the last deglacial including the marshy phase (until ca. 9400 cal. yr BP), marked by diatom absence, and the brackish water lagoon phase (ca. 9400–5900 cal. yr BP), followed by the freshwater lake phase indicated by first appearance of planktonic freshwater *A. ambigua*, *A. granulata*, and *A. subarctica* and the decrease in marine Chaetocerotaceae resting spores and dinoflagellate cysts (Fig. 3). These transitions are also visible in the cluster analysis results of the elemental composition (Fig. 5).

The lithology during the marshy phase (ca. 16,600–9400 cal. yr BP) shows sandy clays with pebbles likely indicating a fluvial depositional environment (Müller et al., 2016; Schmidt et al., 2016). Highest contents of Si and Ti (PC1) represent the terrestrial detritus input at this stage. Generally low Fe contents may be related to low levels of pyrite formation, thus weak marine influence. However, three peaks in Fe (ca. 15,800–15,530, 12,370–12,100, 11,210–10,960 cal. yr BP) accompanied by troughs in Si and/or Ti likely mark phases of marine impact. Diatoms are absent during this phase, except for the three lowermost sample (ca. 16,600–16,250 cal. yr BP) that contains valves of *Diploneis subovalis* Cleve (78%), a common species in running waters (Krammer and Lange-Bertalot, 1997), and *Pinnularia viridis* (Nitzsch) Ehrenberg (15%), reported from a shallow stream-fed pond of only several cm depth (Harper, 1976). Together with the associated lithology (peat), the diatom assemblage might mirror a bog-like environment with calm fluvial discharge conditions at the sampling location before conditions became more unstable in relation to lateglacial environmental changes and a rising sea level, which hindered diatom growth between ca. 16,250 and 9400 cal. yr BP.

LDSZ IIa can be regarded as a transitional zone with characteristics from the marshy and the lagoon phase. In the lower half of LDSZ IIa (ca. 9400–8600 cal. yr BP) the first appearance of benthic freshwater diatoms indicates an early shallow freshwater lake that evolved around

9400 cal. yr BP, which might have been affected by marine influence due to the global relative sea-level rise (Holocene marine transgression) (Chiba et al., 2016). This is shown by coincident appearance of marine diatoms (e.g. *Pinnunavis yarrensis* (Grunow) H. Okuno) and relatively high percentages of *P. brevistriata*, *P. elliptica*, and *Staurosira pinnata* Ehrenberg, which can thrive in slightly brackish waters (Denys, 1990; van Dam et al., 1994). The p-ED-XRF data confirm a marine influence during the lower half of this zone, which is expressed by high loading of PC1 (i.e. higher Fe and lower Si and Ti contents) pointing to a reduced fluvial input. Lower PC1 sample scores, similar to those in LDZ I, and a virtual disappearance of diatoms are recorded in the upper half of LDSZ IIa (ca. 8600–8400 cal. yr BP). We regard this as a phase of re-increased detrital input and weaker marine influence marking a return to more unstable, marsh-like conditions as suggested for LDZ I.

Valves of marine *Cocconeis scutellum*, Chaetocerotaceae, Thalassiosiraceae, and significant peaks in dinoflagellate cyst percentages occur in LDSZ IIb (ca. 8400–5900 cal. yr BP) marking the existence of a brackish water lagoon with tidal influence. The higher Cl contents in the p-ED-XRF data seem to reflect the brackish water conditions because Cl in sediments is often regarded as an indicator for marine influence (Chagué-Goff, 2010). However, the interpretation of Cl is difficult due to its high solubility, which probably is reflected in the relatively large fluctuations of the Cl content within this part of the section. The time around 8400 cal. yr BP may be regarded as the onset of substantial influence of the Holocene marine transgression to the Lake Kushu basin and the beginning of the formation of the sand dune, which, until today, separates the lake from Funadomari Bay.

Freshwater conditions have prevailed during 5900–5100 cal. yr BP (LDSZ IIIa) right after the maximum relative sea level was reached (Chiba et al., 2016). This is indicated by the dominance of planktonic freshwater *A. ambigua*, *A. granulata*, *A. islandica*, Stephanodiscaceae, and benthic Epithemiaceae. Brackish taxa suggest regular influence from the adjacent marine environment that may be due to fluctuating sea levels and incomplete sand dune formation. This is corroborated by the reconstructed water parameters (Fig. 4), which illustrate alternating levels of trophy, pH, P/B ratio, the *Pediastrum* percentages (Fig. 3B), and the geochemical data. It shows a high degree of variability of chemofacies groups between 8300 and 5800 cal. yr BP (12.5 to 9.9 m depth, Fig. 5).

During LDSZs IIIb (5100–2200 cal. yr BP) and IIIc (2200–270 cal. yr BP) a meso- to eutrophic, alkaline freshwater water body existed. There is no indication for significant marine influence. The P/B ratios imply highest lake levels during IIIb and generally lower levels during IIIc, which is corroborated by a trend of decreasing PC2 values (increasing Ca content and decreasing Cl content) towards the core top suggesting progressively decreasing lake levels probably due to continuous sediment accumulation (Schmidt et al., 2016). This may also explain the absence/reduction of diatom valves in the four uppermost sediment sections (Fig. 3) as a result of lowered lake levels that led to enhanced eutrophication conditions and consequently to a reduction in diatom blooms to the benefit of other algal groups (Leng and Barker, 2006).

Different correlations are revealed when comparing the derived multi-proxy dataset with available knowledge about human activities on Rebus Island. The onset of stable freshwater conditions at ca. 5100 cal. yr BP coincided with the establishment of the first Neolithic residential sites on the island (Inui, 2000) during the Hokkaido Middle Jomon culture phase (Weber et al., 2013; Abe et al., 2016). We hypothesize that Lake Kushu was a significant source of freshwater and food for these inhabitants and played a role in the establishment of the earliest known permanent settlements on Rebus Island. According to the pollen-based vegetation reconstruction of the last 6000 years (Leipe et al., 2018), there was no significant impact on the island's natural forests by Middle to Late Jomon (ca. 5000–2250 cal. yr BP), Epi Jomon (ca. 2250–1850 cal. yr BP), and Susuya culture (ca. 1850–1450 cal. yr BP) groups. This situation changed when Okhotsk

culture groups immigrated. Deforestation related to this occupation phase started ca. 1470 cal. yr BP and lasted until ca. 1240 cal. yr BP according to the terrestrial pollen record (Leipe et al., 2018). Interpretation of *Pediastrum* as an indicator for enhanced nutrient input (Fredskild, 1983) due to increased surface runoff (i.e. deforestation) likely paralleled by continuous lake shallowing dates the onset of human impact to ca. 1580 cal. yr BP (Fig. 3A). This is roughly in line with the onset of a prolonged phase of diatom growth reduction (ca. 1660–270 cal. yr BP, Fig. 3) with only few samples (i.e. 3 out of 31 analyzed samples) containing ≥ 300 frustules, which is supportive for such change in limnological conditions.

Although no significant human impact is suggested by the RK12 pollen record and archaeobotanical assemblages from the nearby archaeological site Hamanaka 2 (Leipe et al., 2018), it may be assumed that the lake's trophy level remained high due to continuous sedimentation. Despite the re-increase of diatoms in the uppermost two samples (ca. 340–270 cal. yr BP), there is no indication for a reversal trend in lake status. The assemblages represent a shift towards higher eutrophication levels. At the same time, the chemofacies show a shift towards lower PC2 values reflecting higher Ca, Ti, and Fe contents but lower Cl contents, which may evidence silting-up and an increasing terrestrial influence. This development may be related to intensive deforestation activities by northern Hokkaido Classic Ainu (ca. 350–100 cal. yr BP) populations that may have started as early as ca. 410 cal. yr BP as suggested by the RK12 pollen record (Leipe et al., 2018).

5.2. Ecosystem dynamics during the middle Holocene interval 5600–5200 cal. yr BP

The high-resolution diatom (bi-decadal), aquatic pollen and NPP (bi-decadal), and microfacies (annual to seasonal) analyses of RK12-02-9 open a window into a 400-years interval (between ca. 5640 and 5220 cal. yr BP; 938–848 cm depth) of the middle Holocene providing insights into the limnology of Lake Kushu. The analyzed section is of interest as it represents a sequence of pronounced lamination, marks a phase of major and quick changes in the aquatic system (i.e. the final period of significant marine influence before the shift towards stable freshwater conditions), and covers the termination of the Holocene Thermal Optimum (i.e. onset of Middle Holocene cooling; Wanner et al., 2008) in the study region as suggested by the RK12 terrestrial pollen record (Leipe et al., 2018).

Based on the diatom and microfacies analyses the sedimentary succession can be divided into four main zones depicting an alternation of freshwater conditions (ca. 5640–5610 and 5580–5360 cal. yr BP; LDZ-9 I and III) and phases of enhanced marine influence (ca. 5610–5580 and 5340–5220 cal. yr BP; LDZ-9 II and V) (Fig. 7). The two freshwater phases are characterized by abundances of planktonic *A. ambigua* and *A. granulata*, preferring meso- to eutrophic conditions, while the 'marine intervals' are marked by Chaetocerotaceae abundances in both the diatom samples and microfacies and pronounced decrease in freshwater diatom taxa. In LDZ-9 V marine impact is further supported by the appearance of dinoflagellate cysts showing a small peak (5%) at 860 cm (Fig. 3B). A short-term phase (LDZ-9 IV) of a substantially different diatom composition lasting no longer than about 20 years (ca. 5360–5340 cal. yr BP), which is intercalated between LDZ-9 III and V, is represented by the dominance of *S. hantzschii* Grunow and *D. tenuis*, reflecting enhanced nutrient influx (van Dam et al., 1994) derived from terrestrial resources via Oshonnai River discharge.

Regarding the record of the main aquatic pollen and algae taxa it appears that during periods of enhanced marine influence *Myriophyllum* frequencies are high, while *Pediastrum* values are low and that the opposite trend is evident during freshwater-dominated phases. High percentages of *Myriophyllum* – a plant that grows in shallow water – may be explained by intensive sea-water influx during the flowering season leading to the submergence of the anthers causing more pollen to be

deposited in the lake (Leipe et al., 2018). Interpreting variations in green algae (e.g. *Botryococcus* and *Pediastrum*) abundances is commonly more challenging. They are most commonly related to changes in the concentration of nutrients (Lamb et al., 1999), and *Pediastrum* is often regarded as an indicator of nutrient-rich conditions (Fredskild, 1983). However, the nutrient requirements of *Botryococcus* and *Pediastrum*, which are most commonly found in lake sediments, remains poorly understood and cases in which *Pediastrum* decline is related to nutrient-poor conditions are well documented (Cohen, 2003). In the RK12-02-9 record *Pediastrum* growth seems to be favored by nutrient-rich (i.e. mesotrophic to eutrophic) conditions as indicated by *A. ambigua* and *A. granulata* frequencies (LDZ-9 I and III), although the cause for reduced *Pediastrum* growth (LDZ-9 II and V) appears to be increased salinity levels.

The stepwise increase of *A. subarctica* (ca. 5530–5500 cal. yr BP) and its continuous presence until 5430 cal. yr BP suggests a period of decreased water temperatures during LDZ-9 III. This supports the interpretation of Leipe et al. (2018), who hypothesize that the phase of low terrestrial pollen concentrations between ca. 5540 and 5300 cal. yr BP evidences the onset of the hemispheric Middle Holocene cooling that marks the end of the Holocene Thermal Optimum in the study region. A major shift in diatom assemblages (i.e. change from *A. ambigua* to *A. subarctica* dominance) in concert with accumulation of detrital layers and decrease in total pollen concentration, which was recorded in the Lake Suigetsu (central Japan) sediment core at the onset of the Younger Dryas (Kossler et al., 2011), also support our interpretation. Other hemispheric-scale studies results are temporally in agreement, dating this climate transition to around 5500 (Debret et al., 2007) or 5400 cal. yr BP (Grove, 2004; Solomina et al., 2015).

6. Conclusions

The results of the multi-proxy analysis of the RK12 sediment core provide a continuous record of Lake Kushu's limnological conditions over the last lateglacial and Holocene intervals. In combination with the accurate age-depth model, the high-resolution analyses of diatoms, aquatic pollen and NPP, and p-ED-XRF chemofacies allow precise dating of three phases of lake basin development including a marshy phase (ca. 16,600–9400 cal. yr BP), a lagoon phase (ca. 9400–5900 cal. yr BP), and a freshwater lake phase (between ca. 5900 cal. yr BP and the present). The development of lacustrine conditions within the Lake Kushu basin is closely related to the formation of a sand barrier, which, until today, separates the lake from Funadomari Bay of the Sea of Japan. The sand barrier is evidence of the highest sea-level stands associated with the Holocene marine transgression (ca. 8000–6000 cal. yr BP) and a subsequent sea-level stabilization or even regression during the following 'neoglaciation'.

The results of the high-resolution analyses of core section RK12-02-9 (ca. 5600–5200 cal. yr BP) reveal an alternation of decadal-scale phases of freshwater conditions and enhanced marine influence. In this sequence the stepwise increase of *A. subarctica* confirms the timing of the Holocene Thermal Optimum termination (i.e. the onset of Middle Holocene cooling) in the study region around 5530 cal. yr BP that is also suggested by the terrestrial pollen record from the same sediment core (Leipe et al., 2018).

The current proxy records also provide information regarding past human-environment interactions on Rebus Island. The coincidence between the onset of stable freshwater conditions (ca. 5100 cal. yr BP) and the appearance of the earliest permanent settlements during the Middle Jomon culture phase (ca. 5000–4000 cal. yr BP) point to the significance of Lake Kushu as a valuable source for food and freshwater. On the other hand, there is evidence that human activities influenced the lake evolution. First substantial human impact (deforestation activities) by Okhotsk culture (ca. 1450–950 cal. yr BP) and Classic Ainu (ca. 350–100 cal. yr BP) populations on Rebus Island likely led to enhanced sediment and nutrient input into Lake Kushu resulting in high

eutrophication levels. This, in turn, caused the detected strongly reduced diatom productivity and enhanced green algae growth.

Supplementary data to this article can be found online at <https://doi.org/10.1016/j.palaeo.2018.11.010>.

Data availability

Datasets related to this article can be found online in the Open Access information system PANGAEA at <https://doi.org/10.1594/PANGAEA.889779>.

Acknowledgments

The present study is a contribution to the Baikal-Hokkaido Archaeology Project (BHAP) directed by Prof. Andrzej Weber (University of Alberta, Canada) and Prof. Hirofumi Kato (Hokkaido University, Japan). The palaeoenvironmental research (PI: P. Tarasov) on Rebus Island was initiated as part of the BHAP and financed via the Major Collaborative Research Initiative (MCRI) programme of the Social Sciences and Humanities Research Council of Canada, Japan Society for the Promotion of Science, and collaborating institutions, including the University of Alberta, the German Archaeological Institute (DAI), the Hokkaido University, and the Freie Universität Berlin (FUB). Coring of Lake Kushu and core transportation costs were covered by the Japanese MEXT-Japan Kakenhi research grant no. 21101002 held by H. Yonenobu. S. Müller acknowledges the support of H. Kato, T. Irino, and M. Yamamoto, who provided research facilities during her research stay at Hokkaido University. We greatly acknowledge various help and support to the project from local Ainu and fishermen communities and local governmental organizations. We thank T. Haraguchi (Osaka City University) for providing the bathymetry data of Lake Kushu and A. Kossler (FUB) for initial work on the Rebus Island flora identification. M. Schmidt's work was financed via a BHAP PhD stipend (University of Alberta, 0424634401). We appreciate the financial support of the German Research Foundation (DFG Grants LE 3508/1-1, TA 540/5-1, and TA 540/5-2). We further thank Frank Kutz for technical support during semi-continuous p-ED-XRF analyses, and Prof. Thomas Algeo and one anonymous reviewer for their thorough editorial corrections and useful comments, which helped us to improve this paper.

References

- Abe, C., Leipe, C., Tarasov, P.E., Müller, S., Wagner, M., 2016. Spatio-temporal distribution of hunter-gatherer archaeological sites in the Hokkaido region (northern Japan): an overview. *The Holocene* 26 (10), 1–19.
- Aitchison, J., 1986. The Statistical Analysis of Compositional Data. In: Chapman and Hall. London, New York.
- Battarbee, R.W., Jones, V.J., Flower, R.J., Cameron, N.G., Bennion, H., Carvalho, L., Juggins, S., 2001. Diatoms. In: Smol, J.P., Birks, H.J.B., Last, W.M. (Eds.), *Tracking Environmental Change Using Lake Sediments, Terrestrial, Algal, and Siliceous Indicators*. Vol. 3. Kluwer Academic Publishers, Dordrecht, pp. 155–202.
- Beug, H.-J., 2004. Leitfaden der Pollenbestimmung für Mitteleuropa und angrenzende Gebiete. Verlag Dr. Friedrich Pfeil, München (in German).
- Brauer, A., Casanova, J., 2001. Chronology and depositional processes of the laminated sediment record from Lac d'Annecy, French Alps. *J. Paleolimnol.* 25, 163–177.
- Chagué-Goff, C., 2010. Chemical signatures of palaeotsunamis: a forgotten proxy? *Mar. Geol.* 271, 67–71.
- Chen, X.-Y., Blockley, S.P.E., Tarasov, P.E., Xu, Y.-G., McLean, D., Tomlinson, E.L., Albert, P.G., Liu, J.-Q., Müller, S., Wagner, M., Menzies, M.A., 2016. Clarifying the distal to proximal tephrochronology of the Millennium (B-Tm) eruption, Changbaishan Volcano, northeast China. *Quat. Geochronol.* 33, 61–75.
- Chiba, T., Siguhara, S., Matsushima, Y., Arai, Y., Endo, K., 2016. Reconstruction of Holocene relative sea-level change and residual uplift in the Lake Inba area, Japan. *Palaeogeogr. Palaeoclimatol. Palaeoecol.* 441, 982–996.
- Cohen, A.S., 2003. *Paleolimnology: The History and Evolution of Lake Systems*. Oxford University Press, Oxford.
- Cwynar, L.E., Burden, E., McAndrews, J.H., 1979. An inexpensive sieving method for concentrating pollen and spores from fine grained sediments. *Can. J. Earth Sci.* 16, 1115–1120.
- van Dam, H., Mertens, A., Sinkeldam, J., 1994. A coded checklist and ecological indicator values of freshwater diatoms from the Netherlands. *Neth. J. Aquat. Ecol.* 28,

- 117–133.
- Debrét, M., Bout-Roumazeilles, V., Grousset, F., Desmet, M., McManus, J.F., Massei, N., Sebag, D., Petit, J.-R., Copard, Y., Trentesaux, A., 2007. The origin of the 1500-year climate cycles in Holocene North-Atlantic records. *Clim. Past Discuss.* 3, 679–692.
- Demske, D., Tarasov, P.E., Nakagawa, T., Suigetsu 2006 Project Members, 2013. Atlas of pollen, spores and further non-pollen palynomorphs recorded in the glacial-interglacial late Quaternary sediments of Lake Suigetsu, central Japan. *Quat. Int.* 290–291, 164–238.
- van den Boogaart, K.G., Tolosana, R., Bren, M., 2014. Compositions: Compositional Data Analysis.
- Denys, L., 1990. *Fragilaria* blooms in the Holocene of the Western Coastal Plain of Belgium. In: Simola, H. (Ed.), *Proceedings of the Tenth International Diatom-Symposium – Joensuu, Finland 1988*. Koeltz-Scientific Books, Koenigstein, pp. 397–406.
- Fægri, K., Kaland, P.E., Krzywinski, K., 1989. *Textbook of Pollen Analysis*, 4th edition. John Wiley & Sons, Chichester.
- Fredskild, B., 1983. The Holocene development of some low and high arctic Greenland lakes. *Hydrobiologia* 103, 217–224.
- Geospatial Information Authority of Japan, 2012. Topographic map Funadomari 1:25,000.
- Gibson, C.E., Anderson, N.J., Haworth, E., 2003. *Aulacoseira subarctica*: taxonomy, physiology, ecology and palaeoecology. *Eur. J. Phycol.* 38, 83–101.
- Gibson, C.E., Foy, R.H., 1988. The significance of growth rate and storage products for the ecology of *Melosira italica* ssp. *subarctica* in Lough Neagh. In: Round, F.E. (Ed.), *Algae and the Aquatic Environment*. Biopress, Bristol, pp. 88–106.
- Gill, D., Shomrony, A., Fligelmann, H., 1993. Numerical zonation of log suites and log-facies recognition by multivariate clustering. *Am. Assoc. Pet. Geol. Bull.* 77, 1781–1791.
- Goslar, T., Van Der Knaap, W.O., Kamenik, C., Van Leeuwen, J.F.N., 2009. Free-shape ¹⁴C age-depth modelling of an intensively dated modern peat profile. *J. Quat. Sci.* 24, 481–499.
- Goto, Y., McPhie, J., 1998. Endogenous growth of a Miocene submarine dacite cryptodome, Rebut Island, Hokkaido, Japan. *J. Volcanol. Geotherm. Res.* 84, 273–286.
- Grimm, E.C., 1987. CONISS: a FROTRAN 77 program for stratigraphically constrained cluster analysis by the method of incremental sum of squares. *Comput. Geosci.* 13, 13–55.
- Grimm, E.C., 1991–2011. *Tilia® 1.7.16* [Computer Software] Illinois State Museum. Research and Collection Center, Springfield.
- Grove, J.M., 2004. *Little Ice Ages: Ancient and Modern*, second ed. Vol. 2 Routledge, New York.
- Guiry, M.D., Guiry, G.M., 2015. *AlgaeBase. World-wide Electronic Publication. National University of Ireland, Galway*. <http://www.algaebase.org> (accessed in 2015).
- Harper, M.A., 1976. Migration rhythm of the benthic diatom *Pinnularia viridis* on pond silt (note). *N.Z. Aust. J. Mar. Freshwat. Res.* 10, 381–384.
- Hoelzmann, P., Klein, T., Kutz, F., Schütt, B., 2017. A new device to mount portable energy-dispersive X-ray fluorescence spectrometers (p-ED-XRF) for semi-continuous analyses of split (sediment) cores and solid samples. *Geosci. Instrum. Method. Data Syst.* 6, 93–101.
- Houk, V., Klee, R., Tanaka, H., 2010. Atlas of freshwater diatoms with a brief key and descriptions, part III: Stephanodiscaceae A, *Cyclotella*, *Tertiarius*, *Discostella*. In: Pouličková, A. (Ed.), *Fottea 10* (Supplement). Czech Phycological Society, Prague.
- Igarashi, Y., 2013. Holocene vegetation and climate on Hokkaido Island, northern Japan. *Quat. Int.* 290–291, 139–150.
- Igarashi, Y., Zharov, A.E., 2011. Climate and vegetation change during the late Pleistocene and early Holocene in Sakhalin and Hokkaido, northeast Asia. *Quat. Int.* 237, 24–31.
- Interlandi, S.J., Kilham, S.S., Theriot, E.C., 1999. Responses of phytoplankton to varied resource availability in large lakes of the Greater Yellowstone Ecosystem. *Limnol. Oceanogr.* 44, 668–682.
- Inui, T., 2000. Iseki no ichi to shuhen no kankyo [Site location and environment]. In: Nishimoto, T. (Ed.), *Rebut cho Funadomari Iseki Hakutsu Chosa Hokokusho* [Report on the Excavation at the Site of Funadomari]. Rebut Cho Kyoiku linkai, Rebut, pp. 5–10 (in Japanese).
- Jarvis, A., Reuter, H.I., Nelson, A., Guevara, E., 2008. Hole-filled Seamless SRTM Data V4. International Centre for Tropical Agriculture (CIAT).
- Juggins, S., 2015. *Rioja: Analysis of Quaternary Science Data, R Package Version (0.9-5)*. cran.r-project.org/package=rioja.
- Kilham, S.S., Theriot, E.C., Fritz, S.C., 1996. Linking planktonic diatoms and climate change in the large lakes of the Yellowstone ecosystem using resource theory. *Limnol. Oceanogr.* 41, 1052–1062.
- Kimura, G., 1997. Cretaceous episodic growth of the Japanese Islands. *Island Arc* 6, 52–68.
- Kobayashi, H., Idei, M., Nagumo, T., Mayama, S., Osada, K., 2006. *H. Kobayashi's Atlas of Japanese Diatoms Based on Electron Microscopy*. Vol. 1 Uchida Rokakuho Publishing Co., Ltd., Tokyo (in Japanese).
- Kossler, A., Tarasov, P., Scholout, G., Nakagawa, T., Marshall, M., Brauer, A., Staff, R., Bronk Ramsey, C., Bryant, C., Lamb, H., Demske, D., Gotanda, K., Haraguchi, T., Yokoyama, Y., Yonenobu, H., Tada, R., Suigetsu 2006 Project Members, 2011. Onset and termination of the late-glacial climate reversal in the high-resolution diatom and sedimentary records from the annually laminated SG06 core from Lake Suigetsu, Japan. *Palaeogeogr. Palaeoclimatol. Palaeoecol.* 306, 103–115.
- Krammer, K., Lange-Bertalot, H., 1997. *Bacillariophyceae*. 1. Teil: Naviculaceae. In: Ettl, H., Gerloff, J., Heynig, H., Mollenhauer, D. (Eds.), *Süßwasserflora von Mitteleuropa 2/1*. Spektrum Akademischer Verlag, Heidelberg (in German).
- Krammer, K., Lange-Bertalot, H., 1999. *Bacillariophyceae*. 2. Teil: Bacillariaceae, Epithemiaceae, Surirellaceae. In: Ettl, H., Gerloff, J., Heynig, H., Mollenhauer, D. (Eds.), *Süßwasserflora von Mitteleuropa 2/2*. Spektrum Akademischer Verlag, Heidelberg (in German).
- Krammer, K., Lange-Bertalot, H., 2000. *Bacillariophyceae*. 3. Teil: Centrales, Fragilariaceae, Eunotiaceae. In: Ettl, H., Gerloff, J., Heynig, H., Mollenhauer, D. (Eds.), *Süßwasserflora von Mitteleuropa 2/3*. Spektrum Akademischer Verlag, Heidelberg (in German).
- Krammer, K., Lange-Bertalot, H., 2004. *Bacillariophyceae*. 4. Teil: Achnantheaceae. Kritische Ergänzungen zu *Achnanthes* s. l., *Navicula* s. str., *Gomphonema*. In: Ettl, H., Gerloff, J., Heynig, H., Mollenhauer, D. (Eds.), *Süßwasserflora von Mitteleuropa 2/4*. Spektrum Akademischer Verlag, Heidelberg (in German).
- Kumano, S., Ihira, M., Kuromi, M., Maeda, Y., Matsumoto, E., Nakamura, T., Matsushima, Y., Sato, H., Matsuda, I., 1990. Holocene history of some Coastal Plains in Hokkaido, Japan V. Sedimentary history of Kushu Lake and Akkeshi. *Ecol. Res.* 5, 277–289.
- Lamb, H., Roberts, N., Leng, M., Barker, P., Benkaddour, A., van der Kaars, S., 1999. Lake evolution in a semi-arid montane environment: response to catchment change and hydroclimatic variation. *J. Paleolimnol.* 21, 325–343.
- Lee, J.H., 2011. *Algal Flora of Korea*, Vol. 3, No. 5. Marine Diatoms I: Chrysophyta: Bacillariophyceae: Centrales: Biddulphiineae: Chaetoceraeae. National Institute of Biological Resources, Korea.
- Lee, J.H., 2012. *Algal Flora of Korea*, Vol. 3, No. 6. Marine Diatoms II: Chrysophyta: Bacillariophyceae: Centrales: Thalassiosiraceae: Rhizosoleniaceae. National Institute of Biological Resources, Korea.
- Leipe, C., Kito, N., Sakaguchi, Y., Tarasov, P.E., 2013. Vegetation and climate history of northern Japan inferred from the 5500-year pollen record from the Oshima Peninsula, SW Hokkaido. *Quat. Int.* 290–291, 151–163.
- Leipe, C., Sergusheva, E.A., Müller, S., Spengler III, R.N., Goslar, T., Kato, H., Wagner, M., Weber, A.W., Tarasov, P.E., 2017. *Barley (Hordeum vulgare)* in the Okhotsk culture (5th–10th century AD) of northern Japan and the role of cultivated plants in hunter-gatherer economies. *PLoS One* 12, e0174397.
- Leipe, C., Müller, S., Hille, K., Kato, H., Kobe, F., Schmidt, M., Seyffert, K., Spengler III, R., Wagner, M., Weber, A.W., Tarasov, P.E., 2018. Vegetation change and human impacts on Rebut Island (Northwest Pacific) over the last 6000 years. *Quat. Sci. Res.* 193, 129–144.
- Leng, M.J., Barker, P.A., 2006. A review of the oxygen isotope composition of lacustrine diatom silica for palaeoclimate reconstruction. *Earth Sci. Rev.* 75, 5–27.
- Levkov, Z., 2009. *Amphora sensu lato*. In: Lange-Bertalot, H. (Ed.), *Diatoms of Europe*. Vol. 5 A.R.G. Gantner K.G., Ruggell.
- Lynch, J., 1990. Provisional elemental values for eight new geochemical lake sediment and stream sediment reference materials LKSD-1, LKSD-2, LKSD-3, LKSD-4, STSD-1, STSD-2, STSD-3 and STSD-4. *Geostand. Newslett.* 14, 153–167.
- Miyoshi, N., Fujiki, T., Kimura, H., 2011. *Pollen Flora of Japan*. Hokkaido University Press, Sapporo.
- Montero-Serrano, J.C., Palarea-Albaladejo, J., Martín-Fernández, J.A., Martínez-Santana, M., Gutiérrez-Martín, J.V., 2010. Sedimentary chemofacies characterization by means of multivariate analysis. *Sediment. Geol.* 228, 218–228.
- Müller, S., Schmidt, M., Kossler, A., Leipe, C., Irino, T., Yamamoto, M., Yonenobu, H., Goslar, T., Kato, H., Wagner, M., Weber, A.W., Tarasov, P.E., 2016. Palaeobotanical records from Rebut Island and their potential for improving the chronological control and understanding human–environment interactions in the Hokkaido Region, Japan. *The Holocene* 26, 1646–1660.
- Nakagawa, T., Kitagawa, H., Yasuda, Y., Tarasov, P.E., Gotanda, K., Sawai, Y., 2005. Pollen/event stratigraphy of the varved sediment of Lake Suigetsu, central Japan from 15,701 to 10,217 SG kyr BP (Suigetsu varve years before present): Description, interpretation, and correlation with other regions. *Quat. Sci. Res.* 24, 1691–1701.
- Nakamura, J., 1980a. Diagnostic characters of pollen grains of Japan, part I. In: *Osaka Museum of Natural History* (Ed.), *Special Publications from the Osaka Museum of Natural History*. Vol. 12 Osaka Museum of Natural History, Osaka 91 pp. (in Japanese).
- Nakamura, J., 1980b. Diagnostic characters of pollen grains of Japan, part II. In: *Osaka Museum of Natural History* (Ed.), *Special Publications from the Osaka Museum of Natural History*. Vol. 13 Osaka Museum of Natural History, Osaka 157 pp. (in Japanese).
- Ohtsuka, T., 2002. Checklist and illustration of diatoms in the Hii River. *Diatom* 18, 23–56.
- Olympus Corporation, 2011. *cellSens® Dimension: Release 1.5*. Scientific Research Solution Group, Tokyo, Japan, Hamburg, Germany.
- Palarea-Albaladejo, J., Martín-Fernández, J.A., 2013. Values below detection limit in compositional chemical data. *Anal. Chim. Acta* 764, 32–43.
- Palarea-Albaladejo, J., Martín-Fernández, J.A., 2015. *zCompositions — R package for multivariate imputation of left-censored data under a compositional approach*. *Chemom. Intell. Lab. Syst.* 143, 85–96.
- Patrick, R., 1977. Ecology of freshwater diatoms and diatom communities. In: Werner, D. (Ed.), *The Biology of Diatoms*. University of California Press, pp. 284–332.
- Poister, D., Kurth, A., Farrell, A., Gray, S., 2012. Seasonality of *Aulacoseira ambigua* abundance and filament length: biogeochemical implications. *Plankton Benthos Res.* 7 (2), 55–63.
- R Core Team, 2013. *R: A language and environment for statistical computing*. R Foundation for Statistical Computing, Vienna, Austria. <http://www.R-project.org/>.
- Reille, M., 1992. Pollen et spores d'Europe et d'Afrique du nord. *Laboratoire de Botanique historique et Palynologie*, Marseille.
- Reille, M., 1995. Pollen et spores d'Europe et d'Afrique du nord, Supplement 1. *Laboratoire de Botanique historique et Palynologie*, Marseille.
- Reille, M., 1998. Pollen et spores d'Europe et d'Afrique du nord, Supplement 2. *Laboratoire de Botanique historique et Palynologie*, Marseille.
- Reimer, P.J., Bard, E., Bayliss, A., Beck, J.W., Blackwell, P.G., Ramsey, C.B., Buck, C.E., Cheng, H., Edwards, R.L., Friedrich, M., Grootes, P.M., Guilderson, T.P., Hafldadsson, H., Hajdas, I., Hatté, C., Heaton, T.J., Hoffmann, D.L., Hogg, A.G., Hughen, K.A.,

- Kaiser, K.F., Kromer, B., Manning, S.W., Niu, M., Reimer, R.W., Richards, D.A., Scott, E.M., Southon, J.R., Staff, R.A., Turney, C.S.M., van der Plicht, J., 2013. IntCal13 and Marine13 Radiocarbon Age Calibration Curves 0–50,000 years cal BP. *Radiocarbon* 55, 1869–1887.
- Reuter, H.I., Nelson, A., Jarvis, A., 2007. An evaluation of void filling interpolation methods for SRTM data. *Int. J. Geogr. Inf. Sci.* 21, 983–1008.
- Reynolds, C.S., 1998. What factors influence the species composition of phytoplankton in lakes of different trophic status? *Hydrobiologia* 369 (370), 11–26.
- Rioual, P., Andrieu-Ponel, V., de Beaulieu, J.-L., Reille, M., Svobodova, H., Battarbee, R.W., 2007. Diatom responses to limnological and climatic changes at Ribains Maar (French Massif Central) during the Eemian and Early Würm. *Quat. Sci. Rev.* 26, 1557–1609.
- Sato, H., Kumano, S., Maeda, Y., Nakamura, T., Matsuda, I., 1998. The Holocene development of Kushu Lake on Rebun Island in Hokkaido, Japan. *J. Paleolimnol.* 20, 57–69.
- Schmidt, M., Tarasov, P.E., Hoelzmann, P., Meyer, H., Leipe, C., 2016. Diatoms from Lake Kushu: a pilot study to test the potential of a Late Quaternary palaeoenvironmental archive from Rebun Island (Hokkaido Region, Japan). *J. Asian Earth Sci.* 122, 106–122.
- Shear, H., Nalewajko, C., Bacchus, H.M., 1976. Some aspects of the ecology of *Melosira* ssp. in Ontario lakes. *Hydrobiologia* 50, 73–176.
- Shimakura, M., 1973. Palynomorphs of Japanese plants. In: *Osaka Museum of Natural History* (Ed.), *Special Publications from the Osaka Museum of Natural History* (Osaka, Japan), 60 pp. (in Japanese).
- Solomina, O.N., Bradley, R.S., Hodgson, D.A., Ivy-Ochs, S., Jomelli, V., Mackintosh, A.N., Nesje, A., Owen, L.A., Wanner, H., Wiles, G.C., Young, N.E., 2015. Holocene glacier fluctuations. *Quat. Sci. Rev.* 111, 9–34.
- Stockmarr, J., 1971. Tablets with spores used in absolute pollen analysis. *Pollen Spores* 13, 614–621.
- Stoermer, E.F., Ladewski, T.B., 1976. Apparent Optimal Temperatures for the Occurrence of Some Common Phytoplankton Species in Southern Lake Michigan. Great Lakes Research Division, Publication 18, The University of Michigan, Ann Arbor.
- Strauss, T., von Maltitz, M.J., 2017. Generalizing Ward's method for use with Manhattan distances. *PLoS One* 12 (1), e0168288.
- Tanaka, H., 2014. *Atlas of Freshwater Fossil Diatoms in Japan – Including Related Recent Taxa*. Uchida Rokakuho Publishing Co., Ltd., Tokyo (in Japanese).
- Tarasov, P.E., White, D., Weber, A.W., 2013. The Baikal-Hokkaido Archaeology Project: Environmental archives, proxies and reconstruction approaches. *Quat. Int.* 290–291, 1–2.
- Templ, M., Filzmoser, P., Reimann, C., 2008. Cluster analysis applied to regional geochemical data: problems and possibilities. *Appl. Geochem.* 23, 2198–2213.
- Wanner, H., Beer, J., Bütikofer, J., Crowley, T.J., Cubasch, U., Flückiger, J., Goosse, H., Grosjean, M., Joos, F., Kaplan, J.O., Küttel, M., Müller, S.A., Prentice, I.C., Solomina, O., Stocker, T.F., Tarasov, P.E., Wagner, M., Widmann, M., 2008. Mid- to Late Holocene climate change: an overview. *Quat. Sci. Rev.* 27, 1791–1828.
- Weber, A.W., Jordan, P., Kato, H., 2013. Environmental change and cultural dynamics of Holocene hunter-gatherers in Northeast Asia: Comparative analyses and research potentials in Cis-Baikal (Siberia, Russia) and Hokkaido (Japan). *Quat. Int.* 290–291, 3–20.